Adherens junction remodeling by the Notch pathway in *Drosophila melanogaster* oogenesis

Muriel Grammont

Institut National de la Santé et de la Recherche Medicale, Unité 384; University Clermont 1, Unité de Formation et de Recherche Médecine, Clermont-Ferrand F-63001, France

Identifying genes involved in the control of adherens junction (AJ) remodeling is essential to understanding epithelial morphogenesis. During follicular epithelium development in *Drosophila melanogaster*, the main body follicular cells (MBFCs) are displaced toward the oocyte and become columnar. Concomitantly, the stretched cells (StCs) become squamous and flatten around the nurse cells. By monitoring the expression of epithelial cadherin and Armadillo, I have discovered that the rate of AJ disassembly between the StCs is affected in follicles with somatic clones mutant for *fringe* or *Delta* and *Serrate*. This results in abnormal StC flattening and delayed MBFC displacement. Additionally, accumulation of the myosin II heavy chain Zipper is delayed at the AJs that require disassembly. Together, my results demonstrate that the Notch pathway controls AJ remodeling between the StCs and that this role is crucial for the timing of MBFC displacement and StC flattening. This provides new evidence that Notch, besides playing a key role in cell differentiation, also controls cell morphogenesis.

Introduction

Epithelial cell morphogenesis is a key step in the formation and development of multicellular organisms. Morphogenetic processes involving cell shape change or cell displacement inside an epithelial sheet depend on the flexibility of the cohesiveness between epithelial cells, which is ensured by several adhesion systems, such as the adherens junctions (AJs). Thus, elucidating the regulation of the expression of molecules involved in cellular adhesion is crucial to increasing our knowledge of epithelial cell morphogenesis. The somatic follicular cells of *Drosophila melanogaster* ovarian follicles provide a simple system for studying epithelial morphogenesis. Initially, these cells have a cuboidal shape and form a monolayer around each 16-cell germline cyst. Throughout oogenesis, they progressively differentiate into distinct populations that adopt a squamous or columnar shape and undergo various morphogenetic movements. Thus, studying cell morphogenesis of the follicular epithelium should further our understanding of how cell shape change and cell displacement proceed in an epithelial sheet.

When a follicle leaves the germarium (stage 1), it consists of a germ cyst of 16 cells (one oocyte and 15 nurse cells [NCs]) surrounded by a monolayer of follicular cells (Fig. 1; Spradling, 1993). Three different subpopulations of somatic cells can be identified: the polar cells, the stalk cells, and the follicular cells (Fig. 1 A). Two pairs of polar cells are present at each extremity of the follicle, whereas the interfollicular cells are organized into a stalk of four to six cells that intercalate between adjacent follicles. These two populations play a critical role in follicle formation (Grammont and Irvine, 2001; Lopez-Schier and St Johnston, 2001; Torres et al., 2003). The differentiation of the follicular epithelium starts with the specification of the terminal follicular cells versus the main body follicular cells (MBFCs; Gonzalez-Reyes et al., 1995; Roth et al., 1995). At the anterior pole, the terminal cells give rise to the border cells, the stretched cells (StCs), and the centripetal cells (Fig. 1 A). These three populations cannot be recognized before stage 9 or 10, when specific markers or genes are expressed and several morphogenetic features become apparent (Spradling, 1993; Dobens and Raftery, 2000; Horne-Badovinac and Bilder, 2005). Of relevance to the present study are the morphogenetic processes that concern the MBFCs and StCs: at stage 9, the MBFCs displace toward the oocyte and take on a columnar shape when they make contact with it, whereas the StCs flatten around the NCs to maintain a continuous epithelium. This flattening starts from the most anterior cells and extends progressively to the cells located more posteriorly. This process can be monitored by the expression of the MA33 and *decapentaplegic* (*dpp*) enhancer trap lines and of the Eyes absent protein (Eya; see Materials and methods). At the end of the process of StC flattening, most of

Correspondence to Muriel Grammont: muriel.grammont@inserm.u-clermont1.fr

Abbreviations used in this paper: AJ, adherens junction; A/P, anterior-posterior; ECad, epithelial cadherin; MBFC, main body follicular cell; NC, nurse cell; NCad, Notch cadherin; StC, stretched cell; WT, wild type.

The online version of this article contains supplemental material.

The Journal of Cell Biology, Vol. 177, No. 1, April 9, 2007 139–150
http://www.jcb.org/cgi/doi/10.1083/jcb.200609079

the nuclei of the 50 or so StCs are positioned in the interstitial gaps between the NCs (Fig. 1 B; Spradling, 1993). The rearrangement of MBFCs into columnar cells, their displacement toward the oocyte, and the flattening of StCs are morphogenetic processes that are poorly understood, and the genes involved are almost entirely unknown.

The Notch signaling pathway is required at several stages of oogenesis. First, the Notch receptor is required for polar cell differentiation in the germarium. This entails the germline production of the ligand Delta (Dl) and the specific expression of the Notch modulator Fringe (Fng) in the polar cell precursors (Grammont and Irvine, 2001; Lopez-Schier and St Johnston, 2001; Torres et al., 2003). Second, the Notch signaling pathway is required to induce a transition from the mitotic cycle to the endocycle in follicular cells at stage 6 of oogenesis. This role is also dependent on the germline production of Dl but is *fng* independent (Deng et al., 2001). Third, stage 10 follicles mutant for *Notch* display defects in the differentiation of the border, stretched, and centripetal cells as well as abnormal migration (Gonzalez-Reyes and St Johnston, 1998; Keller Larkin et al., 1999; Zhao et al., 2000; Dobens et al., 2005). Although the first two requirements of *Notch* have been analyzed in detail, the third is poorly defined because it has only been demonstrated using a *Notch* thermosensitive allele. Thus, the precise role of Notch in differentiation of the border, stretched, and centripetal cells and in their morphogenesis remains an unresolved question.

In this study, I have taken a different approach to address this question by analyzing the role of *fng* during StC flattening and MBFC displacement, as its expression pattern from stages 7–10A suggest that it could be involved. Indeed, during these stages, *fng* mRNA is present in all of the follicular cells except the outer border cells (Zhao et al., 2000; Grammont and Irvine, 2001). Somatic mutant clones for an *fng*-null allele (fng^{13}) have been generated, and analysis of the phenotypes induced by the mutant clones leads to the conclusion that the Notch pathway functions in an *fng*-dependent manner to control AJ remodeling between the StCs and that this activity is essential for proper StC flattening and for the timing of MBFC displacement.

Results

fng is required in the StC and the anterior MBFC to control StC number and the timing of MBFC displacement

Because *fng* is required for the differentiation of polar cells, which, in turn, promote terminal cell differentiation (Silver and Montell, 2001; Beccari et al., 2002; Grammont and Irvine, 2002; Xi et al., 2003), only follicles with somatic fng^{13} clones that do not include the anterior and posterior polar cells were analyzed. Only the role of *fng* in MBFC displacement and StC flattening will be analyzed in detail here. In the phenotypic description, references to the MBFC include the cells destined to become centripetal cells because the two cell types are indistinguishable until stage 10 (Fig. 1 A). When fng^{13} clones encompass some StCs and some MBFCs, an excess of cells is observed over the NCs in follicles at stage 10A or older (75%; $n = 60$). As described in the next two paragraphs, these supernumerary cells are either MBFCs or StCs.

In stage 10A follicles, many of the supernumerary cells appear in clusters (Fig. 2 A). These clusters present three traits. First, they display a cell density that is more characteristic of the MBFC population than of the StC population. Second, they are always immediately adjacent to the MBFC population. Third, most of their component cells do not express MA33 or Eya except the ones that are at the anterior border of the cluster (Fig. 2 B), indicating that the majority of these cells do not have a stretched fate. Together, these data suggest that most of the supernumerary cells within these clusters are MBFCs that did not fully complete their displacement. In agreement with this, these clusters are never observed over the NCs at later stages, indicating that they do eventually surround the oocyte (Fig. 2 C). Thus, these observations show that *fng* is required in the StCs and MBFCs to allow the posterior displacement of the MBFCs

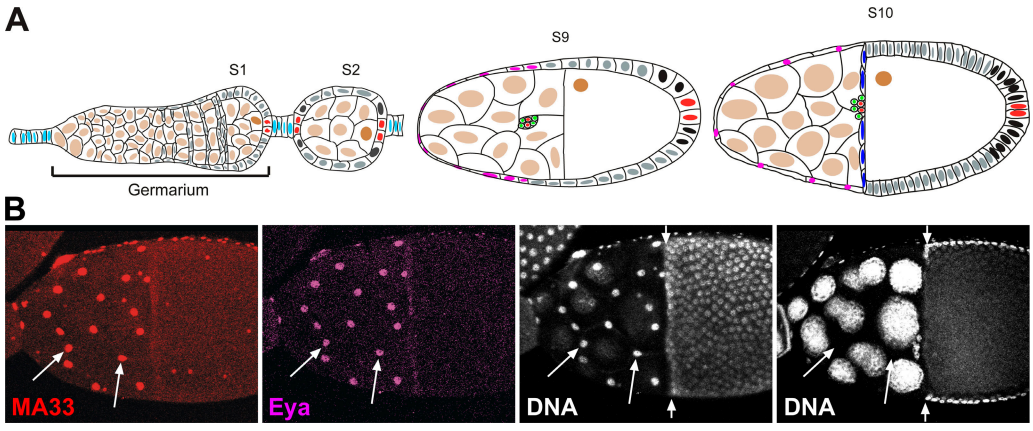

Figure 1. **Schematic of follicular cell populations.** In all figures, anterior is to the left. (A) Schematic of a WT ovariole. The arrangement and identities of the different cells—oocyte (nucleus colored in brown), NC (tan), follicular cells (stage 1) or MBFCs (from stages 2 to 14; gray), polar cells (red), stalk cells (light blue), terminal cells (dark gray), border cells (green), StCs (pink), centripetal cells (dark blue), and posterior cells (black)—are shown in the germarium and in stage 2 (S2), 9 (S9), and 10 (S10) follicles. (B) StC nuclei of the stage 10 WT follicle (long arrows). B′′′ is focused on the medial plane. Short arrows indicate the borders between the oocytes and NCs.

to be fully completed by the end of stage 9. However, because this displacement does still occur, other mechanisms must act in parallel to *fng* to control it.

In stage 10B follicles, supernumerary cells, although no longer arranged in clusters, are still observed over the NCs when a large clone encompasses some MBFCs and some StCs (80%; $n = 25$). These supernumerary cells express every StC marker such as MA33 (Fig. 2 D), Eya (see Fig. 5 A), *dpp-lacZ*, and the Dpp pathway readout *Dad-lacZ*, the latter also being expressed in the StCs during their flattening (see Materials and methods). Thus, all of the supernumerary cells observed over the NCs in stage 10B follicles have an StC fate. As a consequence, in such follicles, the number of StCs increases from ~50 to between 70 and 110 cells (Fig. 2 D). These extra StCs could either have arisen from extra divisions of the fng^{13} cells or from MBFCs that did not get displaced and instead adopted a stretched fate. If these were abnormally proliferating follicular cells, a much higher density of cells would be expected in the part of the mutant clone overlying the NCs, as has been shown for mutant alleles of genes required to stop follicular cell mitotic division (Deng et al., 2001). Moreover, no expression of cyclin B and phosphohistone-3 has been detected in *fng* mutant clones after stage 6 of oogenesis (Deng et al., 2001; unpublished data). Thus, these cells are most likely MBFCs that did not reach the oocyte and differentiated as StCs. In conclusion, the supernumerary cells observed above the NCs at stages 10A and 10B derive from an abnormal displacement of MBFCs.

The penetrance and expressivity of these phenotypes vary based on the type and number of cells that are mutant. The penetrance is higher when the clones encompass both MBFCs and StCs than when they encompass only one of those cell types, showing that *fng* is required in both the StCs and MBFCs. Nevertheless, when the clones encompass just MBFCs, only clones in the anterior part of the MBFC population induce delayed displacement (Fig. 2 E), whereas follicles with a large lateral and/or posterior clone do not (not depicted). This indicates that the requirement of *fng* is different within the MBFC population, with a higher requirement in the anterior cells in contact with StCs. On the other hand, the displacement of MBFCs is more delayed in regions where most of the StCs are mutant than in regions where most of the StCs are wild type (WT), indicating that the StCs play an essential role in MBFC displacement (Fig. 2 F). Finally, MBFC delays are rarely (6%; $n = 30$) observed in small clones (<10 cells; unpublished data), suggesting that the presence of WT cells around the mutant cells prevents it. Equally, some WT MBFCs can be delayed when they are in the immediate proximity of a large clone (Fig. 2 B; see Fig. 5A). This suggests that the process of displacement for one MBFC

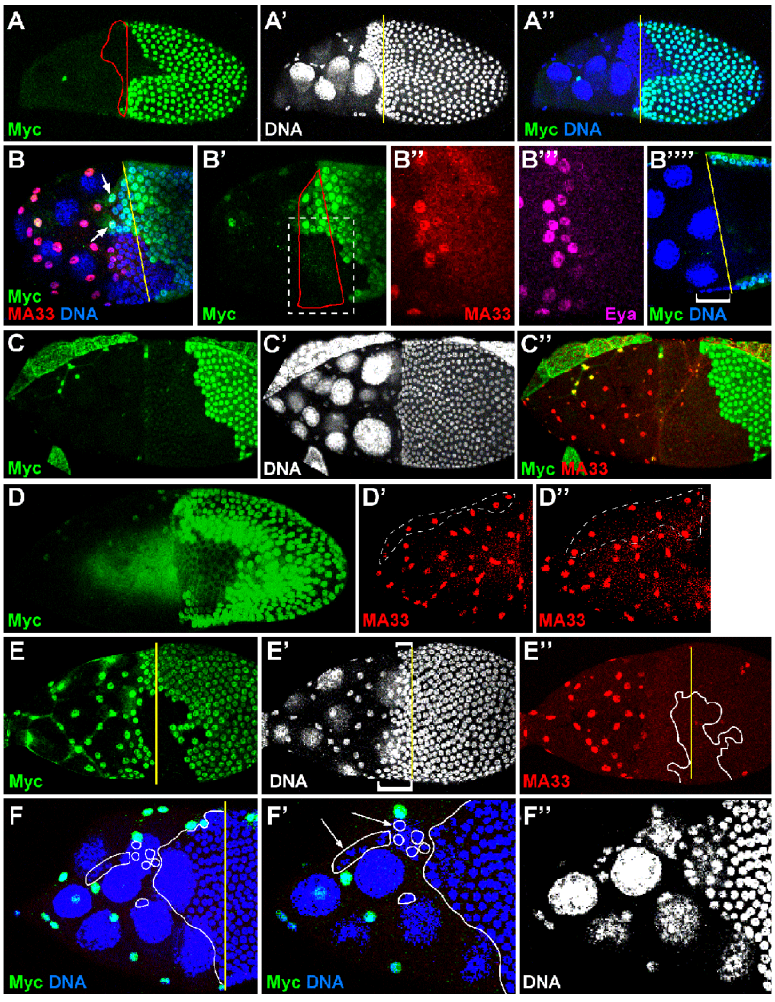

Figure 2. ***fng* is required in the StCs and in the anterior MBFCs to control StC number and the timing of MBFC displacement.** Follicles of stage 10A (A, B, E, and F) or stage 10B (C and D) with fng^{13} clones marked by the absence of Myc. The yellow lines mark the borders between the NCs and oocytes. (A) The cluster of cells (outlined in red) overlying the NC presents a density of nuclei similar to the density of MBFC nuclei. (B) A cluster of cells (outlined in red) with a high density of nuclei overlies the NC. Some cells of the clusters are WT (arrows). B'' and B''' are magnified views on the boxed area in B'. The anterior cells of such clusters express an StC fate (B'' and B'''). B'''' is focused on the medial plane showing some MBFCs overlying an NC (bracket). (C) A follicle with a clone encompassing some StCs and MBFCs. No cluster of cells with a high density overlies the NC. (D) D is a composite view of all of the z sections throughout the follicle, whereas D' and D'' are focused on the top and bottom planes of the follicle, respectively. All of the cells overlying the NC have an StC fate and are 43 and 36 in number in the two focal planes shown (D' and D''). The few WT StCs are outlined with dashed lines. (E) A follicle with a clone encompassing only some MBFCs (outlined in white in E''). More MBFCs overlie the NC in the mutant region (large bracket) than in the WT region (smallbracket). (F) A follicle with a large *fng* clone encompassing most of the MBFCs and a few StCs. An abnormally high number of cells is visible over the NC. F' and F'' are magnified views of the anterior part with a focus on the StC. The mutant cells are outlined in white. MBFCs posterior to WT StCs are less delayed than MBFCs posterior to unflattened mutant StCs (arrows).

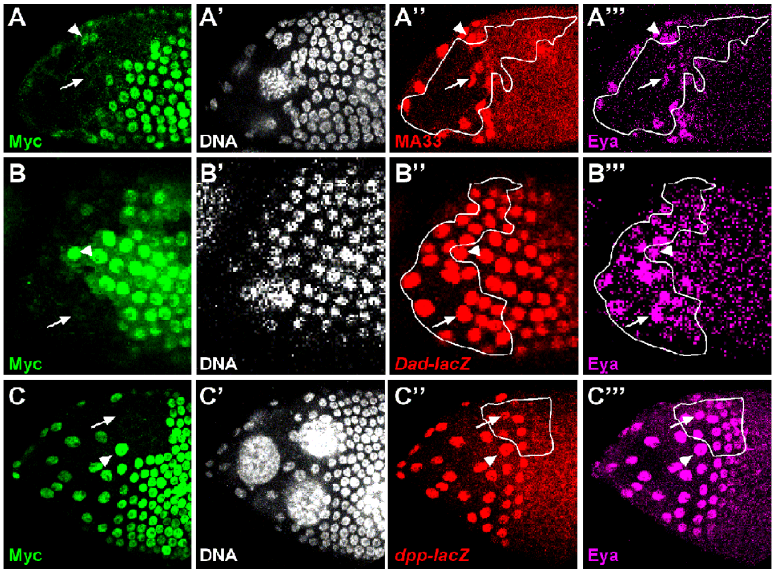

Figure 3. ***fng* is not required for StC differentiation.** Stage 9 follicles with *fng*^{13} clones (outlined in white) spread only over one side of the follicle and marked by the absence of Myc. Expressions of MA33 (A), *Dad-lacZ* (B), *dpp-lacZ* (C), and Eya (A–C) are not affected in mutant cells (arrows) in comparison with WT cells (arrowheads) located at the same A/P position.

depends on the ability of its neighboring cells to be displaced such that the displacement of the MBFC occurs in a coordinated manner all around the follicle and not in a cell-autonomous manner. In conclusion, *fng* is required in the StC and in the anterior MBFC to direct StC number and to control the timing of MBFC displacement.

fng is not required for StC differentiation

It has been proposed that displacement of the MBFC toward the oocyte is the result of cell shape changes of the most posterior cells from cuboidal to columnar, with this change in form forcing their neighboring anterior cells to move posteriorly (Spradling, 1993; Horne-Badovinac and Bilder, 2005). Because no MBFC displacement delay is observed in *fng*^{13} clones encompassing only posterior cells and because no defect in cell shape change has been detected in *fng*^{13} posterior cells, *fng* is not required to generate the force created by the posterior cells (hereafter referred to as the pulling force; unpublished data). In WT follicles, the MBFC displacement probably stops when the StCs are unable to expand any further without compromising the integrity of the epithelium, implying that this displacement also depends on the ability of the cells to respond to the pulling force (for example, by flattening). It is likely, then, that *fng* is involved in this response because a delayed MBFC displacement is observed in most follicles with an *fng*^{13} clone encompassing StCs and anterior MBFCs.

In fact, defective StC flattening and delayed MBFC displacement could arise from a physical inability to undergo morphogenetic processes or from an abnormal StC differentiation (Xi et al., 2003). Accordingly, an analysis of the expression of all known StC fate markers (the Eya protein and the *MA33*, *dpp-lacZ*, and *Dad-lacZ* enhancer traps) has been undertaken in stage 9 follicles containing an anterior clone on one side of the follicle. This provides an internal reference such that marker expression in mutant cells can be compared with WT cells located at the same anterior-posterior (A/P) position. No noticeable difference in the expression of any of the markers was observed between WT and *fng* mutant StCs (Fig. 3, A–C), indicating that differentiation of the *fng* mutant StCs is not delayed in comparison with the WT cells. Moreover, although the role of the Dpp pathway in StC fate determination is unknown, the correct expression of the *Dad-lacZ* enhancer trap in *fng*^{13} StCs rules out the hypothesis that this pathway is not active in these cells (Fig. 3 B). In conclusion, no alteration of StC identity is observed in *fng* mutant follicles.

The Notch pathway controls the dynamics of AJ remodeling

Because the delay in MBFC displacement in *fng*^{13} clones is not caused by a delay in StC differentiation, it leaves open two possibilities: either *fng* mutant StCs are unable to flatten properly and/or *fng* mutant MBFCs cannot move posteriorly properly. One possible underlying cause that could explain both possibilities is a physical inability of the cells to change their shapes and/or to be displaced. Epithelial cell shape change and movement depends on AJ remodeling. A detailed analysis of AJ remodeling was first performed in WT stage 9 follicles because this is as of yet uncharacterized. Because the StCs undergo the greatest cell shape changes within a follicle, it is reasonable to expect that any mutation that causes defects in cell shape changes by modifying the properties of AJs may manifest more dramatically in the StC than in any other cell type.

Therefore, to simplify the study of the role of *fng*, I have chosen to focus on the AJs and their dynamics between the StCs by monitoring the expression of epithelial cadherin (ECad; Fig. 4) and the β-catenin protein Armadillo (Fig. S1, available at http://www.jcb.org/cgi/content/full/jcb.200609079/DC1). The following observations have been obtained from the analysis of a mean of 15 follicles of each stage. Throughout stage 9, a colocalization between the two proteins is observed. In early stage 9 of oogenesis, a strong ECad expression is detected in all follicular cells except the posterior cells. This expression displays the hexagonal shape of the follicular cells, indicating that AJs are present all around each cell close to their apical side (Fig. 4 A).

As a result of the geometry of the cells, some AJs mediate contact between two cells, whereas others mediate contact between three (Fig. 4 A). The orientations of the two-cell junctions are essentially either perpendicular or parallel to the A/P axis. During the process of flattening (midstage 9), no ECad expression is detected at the three-cell junctions that mediate contact between the flattened cells and the flattening cells (Fig. 4 B). In contrast, ECad is still present at the three-cell junctions that mediate contact between the flattening cells and the unflattened cells. Additionally, only a few spots of ECad are observed in the perpendicularly oriented two-cell junctions between the flattened cells and the flattening cells, whereas a strong ECad expression is still observed in those between the flattening cells and the unflattened cells (Fig. 4 B). Distinct patterns are thus observed depending on the degree of flattening of the cells. In late stage 9, most of the AJs are no longer visible except for the ones that are parallel to the A/P axis (Fig. 4 C). At stage 10A, these junctions are barely visible, but ECad starts to be accumulated very strongly in the part of the StC located in the intersticial gaps between NCs. ECad is also detected weakly in the part of the StC overlying the NCs (Fig. 4 D). At stage 10B, the AJs parallel to the A/P axis are no longer detected, but the ECad expression in the part of the StCs overlying the NCs increases, which permits detection of the shape of the StCs. This reveals that most of the StCs are more elongated along the A/P axis than along the dorsal-ventral axis (Fig. 4 E). Identical results for StC shape were also obtained by assaying α-tubulin expression (Fig. 4 F).

To summarize, ECad expression strongly increases just before MBFC displacement and StC flattening. In the StCs undergoing flattening, the three-cell junctions disassemble first, promptly followed by all of the two-cell junctions perpendicular to the A/P orientation and the two-cell junctions parallel to the A/P orientation. This highly dynamic expression permits monitoring of the flattening of StCs and of their shape once the flattening is completed. This ECad expression pattern shows that the process of flattening is coordinated all around the follicle because it starts from the anterior-most row of cells and progresses posteriorly row by row. Finally, the dynamic of this pattern suggests that the order of disassembly of the AJ during stage 9 dictates the direction of cell flattening, allowing the cells to spread and adopt an elongated shape along the A/P axis.

Next, I compared ECad expression patterns in *fng*^{13} mutant StCs to control WT StCs located at the same A/P position within the follicle. At late stage 9, the three-cell junctions between WT cells are disassembled, whereas they are still intact in regions where most of the StCs are mutant (77%; $n = 18$; Fig. 5 A, arrows). The StCs immediately posterior to these latter mutant StCs, whether themselves WT or mutant (Fig. 5 A, long arrow and arrowhead), display ECad staining on all of their edges, indicating that the process of AJ remodeling has not yet started in these cells. Finally, an abnormally high number of StCs as well as a delay in MBFC displacement are observed in the mutant region (77%; $n = 18$). Similar results are obtained by monitoring the expression of Armadillo (75%; $n = 12$; Fig. S1).

Together, these observations show that *fng* is required for the AJ dynamics to occur properly during StC flattening and, thus, that the MBFC displacement delays and the abnormally high number of StCs observed in *fng* mutant follicles derive from a physical inability of the StCs to flatten. ECad expression patterns still differ between mutant and WT regions in a stage 10A *fng*^{13} follicle (Fig. S2, available at http://www.jcb.org/cgi/content/full/jcb.200609079/DC1), but, in late stage 10B follicles, the ECad expression pattern is almost identical between

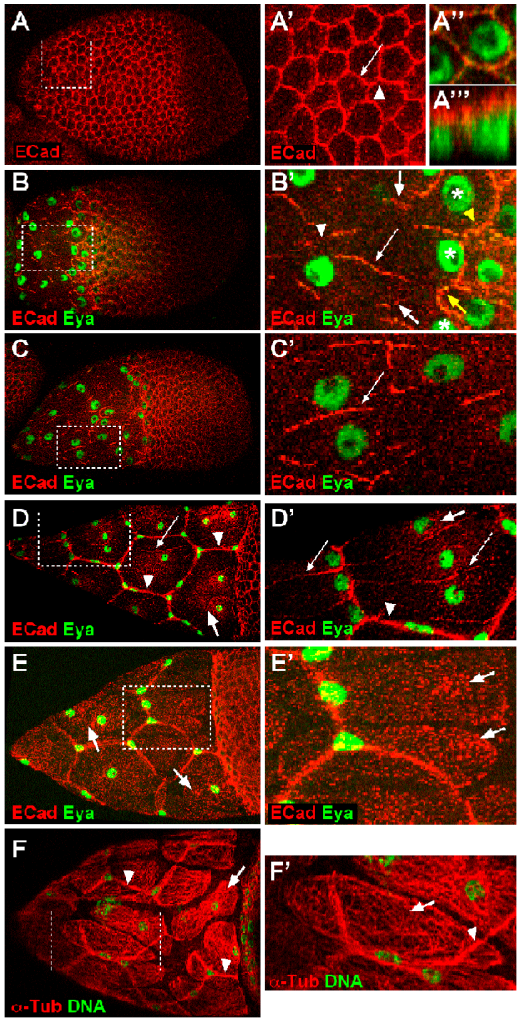

Figure 4. **AJ remodeling in WT follicles.** A′–F′ are magnified views of the boxed areas in A–F. (A) An early stage 9 follicle showing the hexagonally shaped follicular cells that make contact through two-cell (arrow) or three-cell junctions (arrowhead). A′′′ is a z section of the follicular cell shown in A′′. AJs are localized apically (A′′ and A′′′). (B) A midstage 9 follicle. The asterisks indicate the StCs undergoing flattening. ECad is not detected at the three-cell junction between flattened and flattening cells (white arrowhead) but is visible between flattening and unflattened cells (yellow arrowhead). Spots of ECad are present at the perpendicularly oriented junctions between flattened and flattening cells (short white arrows). ECad is strongly detected at the perpendicularly oriented junctions between flattening and unflattened cells (yellow arrow) and at the junctions oriented parallel to the A/P axis (long white arrow). (C) A late stage 9 follicle with most of the AJs parallel to the A/P axis stained (arrow). (D) A stage 10A follicle in which ECad is detected in the part of the StC that is squeezed into the interstitial gaps between NCs (arrowheads). The AJs parallel to the A/P axis are faintly detectable (long arrows), but ECad increases in the part of the StC overlying the NC (short arrows). (E) A stage 10B follicle in which the AJs parallel to the A/P axis are no longer visible. ECad is accumulated in the part of the StC that overlies the NC (arrows). (F) A stage 10B follicle with a tubulin network present in the cytoplasm of the StC that is squeezed into the gaps between NCs (arrowheads) and in the cytoplasm overlying the NCs (arrows).

mutant and WT regions, indicating that AJ remodeling is delayed but not blocked in *fng*^{13} clones (unpublished data). In these follicles, when the majority of the StCs are mutant, there are twice as many StCs as in a WT follicle (Fig. 5 B). Because the overall size of the NC compartment in follicles with many mutant StCs is not substantially different than in WT, each StC likely covers less surface area than a WT (compare Fig. 5 B with Fig. 3 F). Indeed, the mean surface area of an StC in a WT follicle is 1,526 ± 301 μm^2 (n = 30), whereas the mean surface area of an StC in a follicle with a large *fng*^{13} clone is 804 ± 261 μm^2 (n = 83; $P < 0.0001$). This shows that StCs in *fng* mutant follicles flatten less than StCs in WT follicles. In addition, no accumulation of ECad is observed in the part of the StCs that are usually squeezed into the interstitial gaps between the NCs, presumably because the StCs are less flattened and their nuclei are no longer forced into these gaps. In contrast, a higher level of ECad is detected in the part of the StCs overlying the NCs (compare Fig. 5 B with Fig. 4 E). This brighter ECad signal could derive from a higher expression level but more likely reflects the fact that because the cells are smaller, their apical surface is reduced, and, thus, ECad molecules are more concentrated. Staining for α-tubulin yields identical results (Fig. 5, B′ and B′′). In conclusion, *fng* is required for proper flattening of the StCs, which, in turn, controls the minimal number of cells that will adopt this fate.

To address whether this role of *fng* is linked to an activity of the Notch pathway, I conducted a similar analysis with null alleles of *Dl* (*Dl*^{rev10}) and *Ser* (*Ser*^{RX106}). This analysis shows that in stage 9 follicles with anterior clones doubly mutant for *Dl* and *Ser*, most of the three-cell junctions are still present in the mutant region but are disassembled in the WT region (91%; n = 23; Fig. 5 C). Furthermore, an increased density of StCs and a delayed MBFC displacement are observed in the mutant region (Fig. 5 C). No defects have been observed for single *Ser*$^{rev2\text{-}11}$ clones (n = 8), whereas single *Dl*^{rev10} clones yielded similar defects with a weaker expressivity to the double *Dl Ser* mutant clones (87%; n = 15; unpublished data). In addition, as described for *fng*^{13} follicles, the appearance of StC markers occurs properly in the *Dl Ser* mutant StC (unpublished data). Together, these data demonstrate that although the Notch pathway appears not to affect StC identity, it does have an *fng*-dependent role in remodeling their AJs, with *Dl* playing an essential role in the soma and *Ser* having an overlapping function.

A detailed analysis of the expression pattern of Notch and Dl during stage 9 reveals that these two proteins are strongly expressed in the flattened and flattening StCs. In particular, a strong accumulation of Notch is detected at the disassembling three-cell junctions, suggesting that this expression corresponds to the role of Notch described in this study (Fig. 5, D and E). Similarly, analyses of the expression patterns of some reporters for Notch activation show that they are more strongly expressed in the flattened and flattening StCs than in the MBFCs (Fig. S3, available at http://www.jcb.org/cgi/content/full/jcb.200609079/DC1). Thus, the expression patterns of these markers indicate that

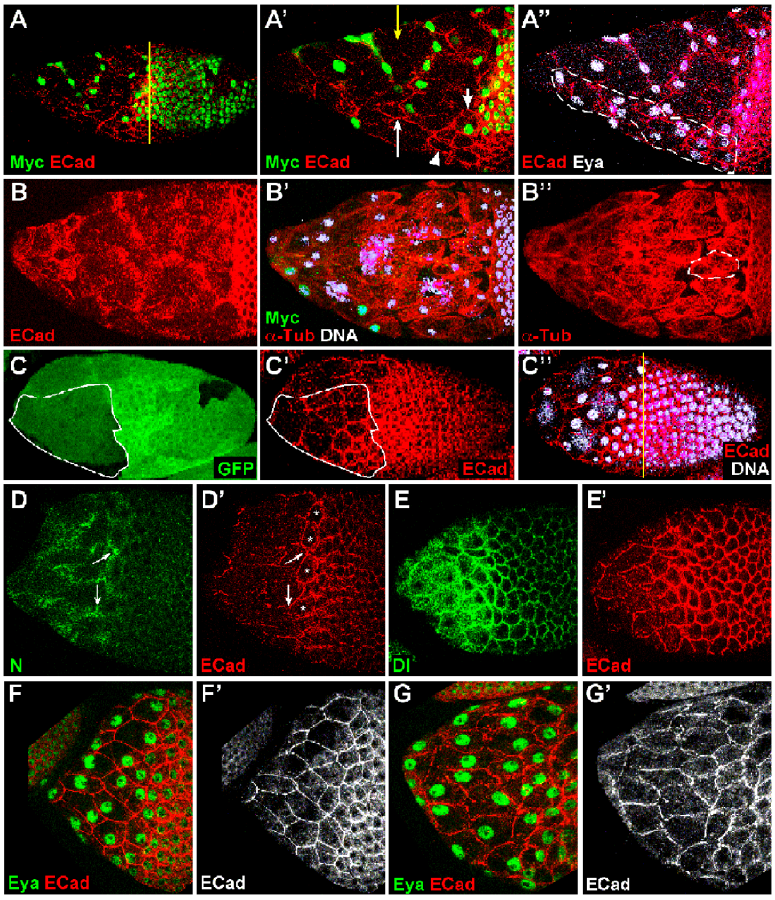

Figure 5. **The Notch pathway is required for the dynamics of AJ remodeling.** The yellow lines mark the borders between the NCs and oocytes. (A and B) Follicles with *fng*^{13} clones marked by the absence of Myc. (A) A late stage 9 follicle with an *fng* clone encompassing some StCs and MBFCs. A′ and A′′ are magnified views of the anterior part of the follicle shown in A. The three-cell junctions are disassembled in the WT region (yellow arrow) but are still present in the mutant region (long arrow). More posteriorly, ECad is still present all around the edges of the cells in the mutant region (arrowhead). A WT cell also displays this pattern (short arrow). More StCs differentiated in the mutant region (outlined in white), and MBFC displacement is delayed. (B) A stage 10B follicle with a large *fng*^{13} clone. An abnormally high number of StCs is observed, and the surface area of one of them is outlined in white. (C) A stage 10A follicle with a *Dl*^{rev10} *Ser*^{RX106} clone marked by the absence of GFP and encompassing some StCs and MBFCs (outlines in white). GFP expression is also visible in the germline cells. Also apparent are delays in MBFC displacement and AJ remodeling. (D and E) WT follicles. The flattening StCs are marked with asterisks. Notch is specifically accumulated at the disassembling three-cell junctions (arrows). (F and G) Follicles overexpressing *Hairless*. (F) No AJ disassembly is detected in an early midstage 9 follicle. (G) Some three-cell–type junctions are disassembling in some StCs in a mid- to late stage 9 follicle.

the Notch pathway is transcriptionally active in the StCs at stage 9. As a direct involvement of the canonical Notch pathway cannot be analyzed (because of its requirement at earlier steps of oogenesis), I tested the effects of overexpressing Hairless, a repressor of Notch transcriptional activity, using an *hs-Hairless* construct. In all stage 9 follicles overexpressing Hairless ($n = 28$), abnormal AJ remodeling is observed. In contrast to WT follicles, no AJ disassembly is detected between StCs in early midstage 9 follicles overexpressing Hairless (compare Fig. 4 B with Fig. 5 F). Rather, this disassembly commences only in mid- to late stage 9 follicles after several rows of StCs have differentiated (Fig. 5 G and Fig. S3 E). This indicates that the transcriptional activity of Notch plays a crucial role in controlling the dynamics of AJ disassembly between StCs at stage 9 of oogenesis.

Follicles expressing a constitutively activated form of Notch (Nact) were then analyzed. Surprisingly, the overexpression of Nact in some StCs leads to an autonomous, abnormal flattening of StCs and a delay in AJ remodeling (72%; $n = 20$; Fig. S3). The shape of Nact-expressing cells remains cuboidal longer than the cells undergoing flattening that are located at the same position along the A/P axis (Fig. S3 F). In parallel, AJ remodeling is delayed in the Nact-expressing region in comparison with the WT region (Fig. S3 G). This indicates that some Notch target genes are involved in AJ remodeling. One could suggest that the loss or gain of activity of the Notch pathway affects the expression of different target genes or that the timing of Notch activation has to be controlled very precisely to allow proper AJ remodeling.

The Notch pathway controls the localization of myosin II

The chronology of AJ disassembly is essential for StC flattening and the timing of MBFC displacement. This chronology likely depends on local effectors at the cell junctions undergoing disruption. The myosin II heavy chain and regulatory light chain, which are encoded by the *zipper* and *spaghetti squash* (*sqh*) genes, respectively, are two effectors that have been shown to remodel cell junctions in a polarized manner (Bertet et al., 2004). To determine whether these two proteins are involved in junction disassembly during StC flattening, their expression patterns were determined in stage 9 follicles. A detailed analysis during stage 9 shows that Zipper is more strongly accumulated in some specific spots, which correspond to disassembling AJs. Indeed, depending on the degree of the flattening of StCs, Zipper can be strongly accumulated along a lateral line that separates the flattened cells from the ones that are flattening (Fig. 6 A). Some parts of this line of expression correspond to the edges of the StCs that are oriented perpendicularly to the A/P axis. Anterior to this line, Zipper is accumulated in StCs both in the vicinity of their nuclei as well as along those edges that are parallel to the A/P axis. In some follicles, this line is not detected, but, instead, a strong accumulation is detected at the disassembling three-cell junctions that are between the row of flattening StCs and the row of unflattened cells (Fig. 6 B). A similar pattern of expression is observed with an Sqh-GFP fusion protein (Fig. 6 C). Together, these observations suggest that these are good candidate proteins for control of the chronology of AJ remodeling during StC flattening.

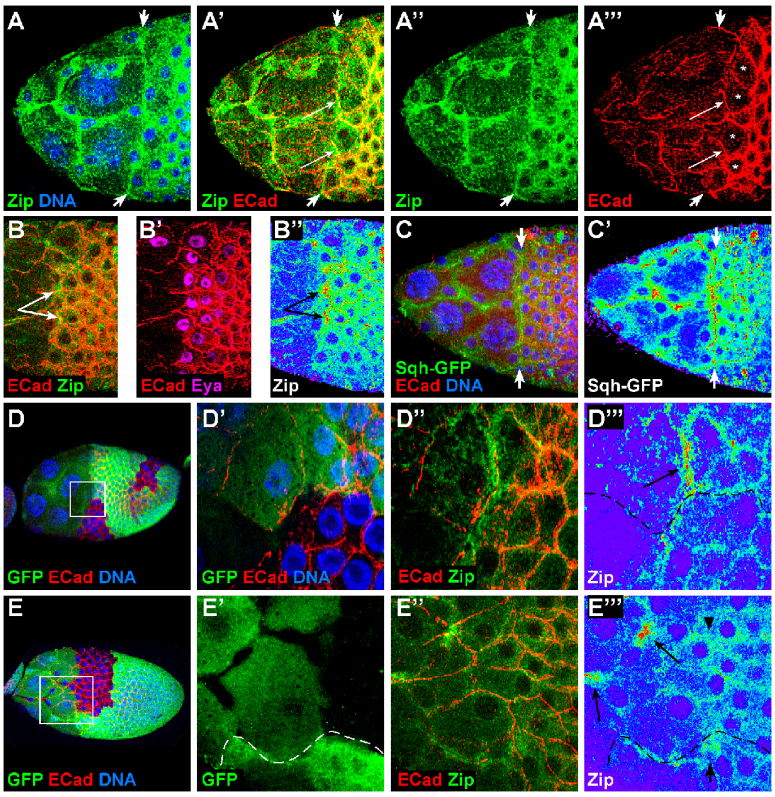

Figure 6. **The Notch pathway controls the localization of myosin II.** The use of a color gradient allows the visualization of differences in intensities of accumulation from none (black) to strongest (red). (A–C) Midstage 9 WT follicles. (A) A line of Zipper expression (flanked by short arrows) perpendicular to the A/P axis is detected at the boundary between flattened and flattening StCs (marked with asterisks). This line comprises some of the junctions that are perpendicular to the A/P axis (long arrows). (B) Zipper is accumulating more strongly at the three-cell junctions between flattening and unflattened StCs (arrows). (C) Sqh-GFP expression. A line of Sqh-GFP expression (flanked by arrows) perpendicular to the A/P axis is detected at the boundary between flattened and flattening StCs. (D and E) Follicles with Dl^{rev10} Ser^{RX106} clones marked by the absence of GFP. MBFC displacement is delayed in the mutant region (D and E). D′–D‴ and E′-E‴ are magnified views of the boxed areas in D and E. (D) Zipper is strongly accumulated along a line perpendicular to the A/P axis in the WT region (arrow), which stops at the boundary of the mutant clone (outlined in black). (E) Zipper is strongly accumulated at disassembling three-cell junctions in the WT region (short arrow). No accumulation of Zipper is detected in the mutant region at the same A/P position (arrowhead), but an accumulation is detected more anteriorly (long arrows). The boundary between WT and mutant regions is outlined in white (E′) or black (E‴).

To confirm this, Zipper expression has been investigated in *Dl Ser* double-mutant follicles. In such follicles, when the lateral line of Zipper accumulation is observed in WT regions, it appears to be interrupted in regions containing mutant cells (Fig. 6 D). Moreover, at the A/P position where Zipper is accumulated at the disassembling three-cell junctions in WT regions, no accumulation is detected in mutant regions (Fig. 6 E). Such accumulations are instead detected at disassembling three-cell junctions located more anteriorly. Thus, the delay in AJ disassembly observed in Dl^{rev10} Ser^{RX106} cells is coincident with the delay in the appearance of Zipper accumulation at disassembling junctions. A similar delay is observed in fng^{13} cells (unpublished data). Thus, the defects in StC flattening and MBFC displacement delay may be caused by a lack of polarization of Zipper during cell junction disassembly.

ECad and myosin II are required for StC flattening

As an impaired Notch pathway results in abnormal delay in AJ remodeling and the modification of Zipper expression pattern during StC flattening, it suggests a role for *shg*, *zipper*, and *sqh* during this process. To test this, somatic mutant clones for an *shg*-null allele (shg^{R69}) and for an *sqh* hypomorphic allele (sqh^{1}) were induced. Stage 9 follicles with *shg* mutant clones display a higher density of flattening StCs in the mutant region than in WT ($n = 12$; Fig. 7, A–A′′). At stage 10, a delay in MBFC displacement is also detected in the mutant region ($n = 10$; Fig. 7 B). Thus, as observed in follicles with *fng* and *Dl*/*Ser* mutant clones, the ability of the StCs to flatten and the timing of MBFC displacement are impaired in *shg* mutant follicles. One might expect that the absence of *shg* would result in the loss of AJs and that StC flattening would occur faster and/or without any constraint. In light of this, the data from the *shg* clones could suggest that the cells are still adhesive. As another adhesion molecule, Notch cadherin (NCad), can also be a component of AJs, its expression was investigated in such clones. In WT follicles, NCad is strongly expressed in all follicular cells from stages 1 to 6 (Fig. 7 C). Its expression decreases during stages 7 and 8 to become almost undetectable at stage 9, with a weak expression in the follicular cells that surround the oocyte and in the StCs (Fig. 7 D). In stage 7–9 follicles with *shg* mutant clones, a strong NCad expression is detected in the mutant cells. This overexpression is cell autonomous in stage 7 follicles ($n = 11$) but is restricted to the anterior part of the clones in stage 8 ($n = 9$) and stage 9 follicles (75%; $n = 20$; Fig. 7, A′′′ and A′′′′; and Fig. S4, available at http://www.jcb.org/cgi/content/full/jcb.200609079/DC1). This overexpression of NCad is no longer detected at stage 10A ($n = 25$; unpublished data). Thus, the absence of ECad is compensated for by the upregulation of NCad from stages 7 to 10 and leads to delayed StC flattening and MBFC displacement, indicating that the levels of ECad and NCad expression during mid-oogenesis are interrelated and that the regulation of ECad expression is important for StC flattening.

The requirement of myosin II cannot be tested directly by using null alleles of *zipper* or *sqh*, as mutant cells will be unable to divide. Thus, a hypomorphic allele of *sqh* was used, and only small clones can be analyzed. In stage 9 follicles, the *sqh* mutant StCs undergoing flattening present an abnormal pattern of ECad. The AJs are not remodeled according to the pattern described for WT cells (Fig. 7 E). Elongation of the mutant cells does not appear to occur mainly along the A/P axis but is more

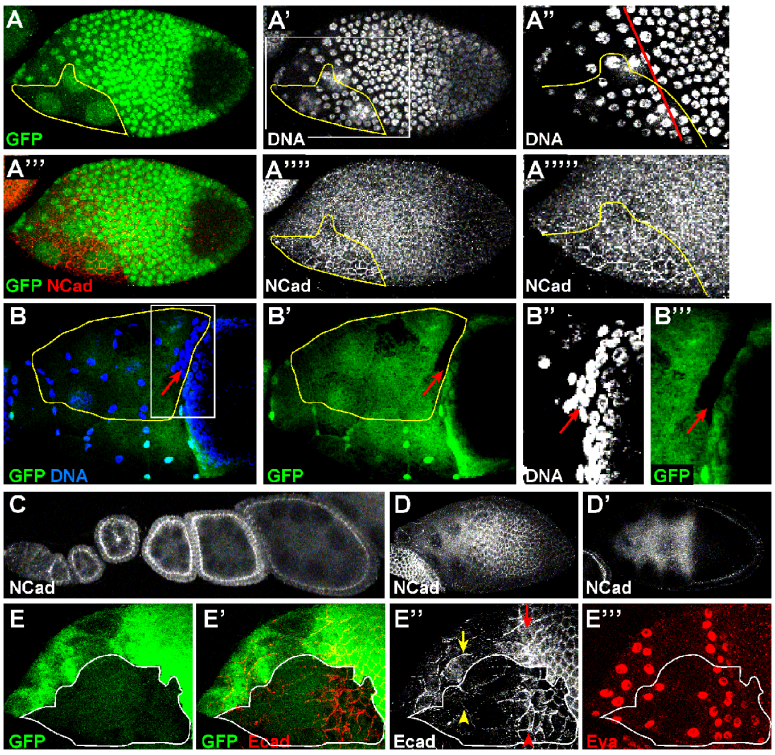

Figure 7. **ECad and myosin II are required for proper StC flattening, the timing of MBFC displacement, and AJ remodeling.** All clones are outlined in yellow in A and B and in white in E. In C and D′, the focus is on the medial plane. (A and B) Follicles with shg^{R69} clones, which are marked by the absence of GFP, encompass some StCs and some MBFCs. (A) A mid-stage 9 follicle with a higher density of StCs in the mutant region. A higher expression of NCad is observed in the mutant clone. A′′ and A′′′′′ are magnified views of the boxed area in A′. The red line marks the border between flattening and unflattened StCs. (B) A stage 10A follicle with delayed MBFC displacement (arrows) in a mutant region. B′′ and B′′′′ are magnified views of the boxed area in B. (C and D) WT ovariole (C) and stage 9 follicle (D) stained for NCad. (E) Stage 9 follicle with an sqh^{1} clone marked by the absence of GFP and encompassing some StCs and some MBFCs. The elongation of the cells (red arrow in mutant and red arrowhead in WT) is no longer oriented in the mutant region, and the AJs parallel to the A/P axis between mutant cells that have already flattened are no longer visible (yellow arrow compared with yellow arrowhead in WT).

randomly oriented. In addition, the AJs parallel to the A/P axis between cells that have already flattened are no longer visible in the mutant region when compared with the WT region. This indicates that activity of the regulatory light chain of myosin II is required to control the dynamic of AJ remodeling and proper StC flattening.

Discussion

Three important morphogenetic events occur in the follicular tissues at stage 9 of oogenesis: border cell migration, StC flattening, and MBFC displacement. My results have advanced the understanding of StC flattening and MBFC displacement in two crucial ways. First, they demonstrate that the rate of MBFC displacement depends on proper StC flattening, which supports the idea that these processes occur in a coordinated manner. Second, they identify the Notch pathway as playing an essential role in StC flattening. In addition to these new insights into follicular cell morphogenesis, my results also demonstrate that the Notch pathway acts during these morphogenetic events by controlling the dynamic of AJ disassembly and not cell identity.

StC differentiation and flattening

It has been previously shown that StC differentiation is a prerequisite for flattening (Xi et al., 2003). My data now show that differentiation is at least partly independent of flattening because differentiation is still occurring in follicles with *fng* or *Dl Ser* mutant clones presenting impaired StC flattening. Surprisingly, in such follicles, supernumerary StCs differentiate, which indicates that the number of cells fated to become StCs is not determined until late stage 9 and that the identity of the centripetal cells and the MBFCs are flexible. It is likely that in *fng* or *Dl Ser* mutant follicles, more cells differentiate and flatten to compensate for the abnormal flattening of the mutant StCs to maintain the integrity of the epithelium. This indicates that the number of StCs per follicle depends on their ability to flatten and on the size of the NC compartment, which is itself variable. The flexibility of the terminal cell population acquiring cell identity has previously been shown for border cell differentiation (Niewiadomska et al., 1999). Thus, although terminal cell differentiation is a prerequisite for morphogenesis, the two processes may be dependent on each other.

Forces controlling StC flattening and MBFC displacement

No cellular or molecular link has ever been established between border cell migration, StC flattening, and MBFC displacement. It has been proposed that the displacement of MBFCs toward the oocyte starts within the posterior cells, which, by adopting a columnar shape, pull their anterior neighbors over the oocyte. As soon as these neighboring cells contact the oocyte, they, in turn, adopt a columnar shape and pull on their anterior neighboring cells (Spradling, 1993; Horne-Badovinac and Bilder, 2005). This process is helped by the growth of the oocyte. My results improve upon this model (Fig. 8), particularly by demonstrating that (1) MBFC displacement depends on the capacity of the StC to flatten and that (2) this flattening depends on the pulling force generated by the posterior cells (3) and on forces generated by each StC, which are referred to as local forces. These points are discussed individually in the following paragraphs.

That MBFC displacement depends on the capacity of the StC to flatten is shown by three lines of evidence. First, MBFC displacement delays are observed in follicles in which *fng* or *Dl Ser* mutant clones encompass only or mainly the StC. Second, the expressivity of this phenotype within a follicle depends on the proportion of the StCs that are mutant. Third, MBFC displacement delays are always detected in *fng* or *Dl Ser* mutant follicles that display abnormal dynamics in AJ disassembly in the StC.

Support for the suggestion that StC flattening depends on the pulling force created by the posterior cells comes first from previous observations of StC behavior in *karst* mutant follicles and in *dicephalic* (*dic*) mutant follicles. In *karst* follicles, as the

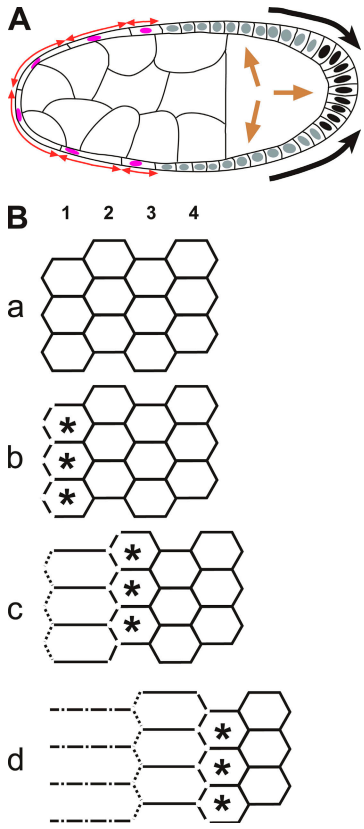

Figure 8. **Model of the morphogenesis of the follicular cells.** (A) Schematic of a stage 9 follicle. The different populations of somatic cells (StCs [nuclei in pink], MBFCs [gray], and posterior cells [black]) are shown as well as the forces involved in StC flattening and MBFC displacement (pulling force [black arrows], oocyte growth [brown arrows], and local forces [red double arrows]). (B) Schematic of AJ disassembly in StCs during stage 9. The AJs of four rows of three StCs are represented at various stages of flattening. The asterisks mark the flattening StCs. (a) Before flattening, the cells have a hexagonal shape. (b) In row 1, the anterior three-cell junctions are disassembling. (c) In row 1, the anterior two-cell junctions perpendicular to the A/P axis are disassembling as well as the three-cell junctions between rows 1 and 2, allowing elongation of the cells along the A/P axis. The junctions parallel to the A/P axis of row 1 are intact. (d) In row 1, the cells are fully flattened. Their junctions parallel to the A/P axis are still present. The two-cell junctions perpendicular to the A/P axis between rows 1 and 2 are disassembling, and the three-cell junctions between rows 2 and 3 are disassembled.

posterior cells do not adopt a columnar shape, it is proposed that the StCs do not flatten because the pulling force is not generated (Zarnescu and Thomas, 1999). In *dic* follicles, the oocyte lies in the middle, with NCs on either side surrounded by anterior terminal cells at the two extremities. Because of the position of the oocyte, the posterior end of the follicle is in the middle, and the two extremities are both anterior ends (Lohs-Schardin, 1982; Gonzalez-Reyes et al., 1997; Gonzalez-Reyes and St Johnston, 1998). At stage 9, the cells that are in contact with the oocyte become columnar and presumably create the pulling force that acts on the StCs located on both sides of the oocyte to guide their flattening. Second, the shape of the StCs after they have flattened in WT follicles is more elongated along the A/P axis than along the dorsal-ventral axis. This reveals that the direction of the elongation of the cells is not random but is instead most likely a consequence of the localization of the pulling force.

The final point is that the capacity of the StC to flatten depends on local forces. Indeed, the shape of the StCs and their coordinated flattening are dependent on the pattern of AJ disassembly at stage 9. This pattern, with the three-cell junctions disassembling first followed by the AJ becoming oriented perpendicularly rather than parallel to the A/P axis of the follicle (Fig. 8), exerts constraints on the cells and prevents them from flattening in a uniform and nondirectional manner. If this cell-autonomous activity is impaired, the StCs do not flatten properly, and the flattening that does occur is no longer coordinated around the follicle, as observed in *fng* or *Dl Ser* mutant follicles. Thus, StC flattening depends, in part, on the cell-autonomous ability of each StC to control AJ disassembly. This control can be a response of the cells that sense and integrate the mechanical strain exerted by the pulling force or can occur independently of the action of the pulling force. Finally, as any force involves regulation of the actin network, the observation that two proteins linking to the actin cytoskeleton (ECad and myosin II) are required for proper StC flattening supports the existence of local forces.

In conclusion, the flattening of StCs is driven by the pulling force and local forces, which together facilitate AJ disassembly in a polarized manner. As a result, both forces coordinate the rate of StC flattening and orient its direction. In parallel, these two forces, along with the growth of the oocyte, define the rate of MBFC displacement. Thus, MBFC displacement and StC flattening are morphogenetic processes that are linked at a cellular level.

The Notch pathway controls the dynamics of AJ remodeling

In contrast to the well-studied role of *Notch* in cell identity determination, the data presented here provides, to my knowledge, the first example in which the Notch pathway is described as playing a role in AJ disassembly and raises the question of whether this role can be extended to other biological contexts. Previous analyses have reported a requirement of *Notch* during late oogenesis using the $Notch^{ts1}$ allele (Gonzalez-Reyes and St Johnston, 1998; Keller Larkin et al., 1999; Zhao et al., 2000; Dobens et al., 2005), but none of them have established its precise function. In this study, I demonstrate that an *fng*-dependent Notch activity is required in the StCs and in the most anterior MBFCs at stage 9 of oogenesis for StC flattening and to control the timing of MBFC displacement. Moreover, the higher accumulation of Notch at disassembling junctions relative to intact junctions in the StCs at the exact moment that disassembly is required supports the fact that the role for Notch in StC flattening is directly related to this specific and strong accumulation. Finally, the pattern of expression of reporters of Notch activation and the defects observed when *Hairless* is overexpressed in the StC indicate that Notch acts in these processes through the canonical pathway. However, as I failed to detect any alterations in cell identity, it is possible that the differentiation defects observed with the $Notch^{ts1}$ allele are caused by its earlier requirement in the arrest of follicular cell mitotic divisions at stage 6 (Deng et al., 2001). Alternatively, the differentiation of some of the terminal populations might be affected by clones encompassing more or different follicular cells than the ones I have focused on in this study. Extensive clonal analyses of *Dl Ser* mutant clones should help resolve this issue.

Activation of the local forces or modifications of the expression and/or localization of adhesion molecules could either be responses to the pulling force or could occur independently of it. Thus, one of the major keys to understanding the role of Notch in AJ disassembly is to determine whether Notch acts on the reception and/or integration of the pulling force or directly on the generation of local forces and on control of the expression and/or localization of adhesion molecules. As for the possibility that Notch controls local forces, it is striking that Zipper accumulation is delayed at the AJ that should have been disassembled in *Dl Ser* mutant clones. Indeed, a recent study has shown the importance of the accumulation of Zipper and Sqh at disassembling junctions for cell intercalation during germband elongation in the *Drosophila* embryo (Bertet et al., 2004). During this process, AJ remodeling occurs with a very specific ordered pattern, and the localization of myosin II mirrors this pattern. Bertet et al. (2004) also show that disrupting myosin II activity genetically or chemically leads to an absence of indicators of AJ remodeling and defects in cell intercalation. In light of these observations, my data suggest a model for AJ disassembly during StC flattening in which the Notch pathway acts on the generation of local forces by controlling a polarized accumulation of Zipper, which, in turn, remodels AJs between the StCs (Fig. 8). How Notch controls the localization of myosin II and how myosin II remodels AJs locally remains to be determined. Finally, the persistence of NCad expression after stage 7 in *shg* mutant clones supports the hypothesis that control of the expression and/or localization of adhesion molecules is through multiple routes.

Materials and methods

Drosophila stocks and crosses

fng^{13}, Dl^{rev10}, $Ser^{rev2\text{-}11}$, Ser^{RX106}, and shg^{R69} are null alleles (Heitzler and Simpson, 1991; de Celis et al., 1993; Irvine and Wieschaus, 1994; Sun and Artavanis-Tsakonas, 1996; Godt and Tepass, 1998), and sqh^{1} is a hypomorph allele (Karess et al., 1991). Canton-S was used as WT, and the reporter lines used were sqh^{AX3}; P(w^{+}, SqhGFP)40 (Royou et al., 2002), *MA33* (Gonzalez-Reyes and St Johnston, 1998), *dpp-lacZ* (Jiang and Struhl, 1995), *Dad-lacZ* (Kai and Spradling, 2003), *Dl-lacZ* (Grossniklaus

et al., 1989), *E(spl)mβ7-lacZ* (an enhancer trap in the *E(spl)mβ7* gene; gift of S. Bray, University of Cambridge, Cambridge, UK), and *E(spl)mβ-CD2* (Cooper and Bray, 1999). *sqh*^{1}, *shg*^{R69}, *fng*^{13}, *Dl*^{rev10}, *Ser*$^{rev2\text{-}11}$, and *Dl*^{rev10} *Ser*^{RX106} clones were generated by Flipase-mediated mitotic recombination on FRT101, FRT42D, FRT80-3, or FRT82B chromosomes and was marked using *π-Myc* or *GFP* transgenes (Xu and Rubin, 1993). Ectopic expression of activated Notch was performed by generating Flip-out Gal4 clones in animals carrying UAS-ΔN34a (Doherty et al., 1996) and *AyGal4 UASGFP* (Ito et al., 1997) transgenes. Flipase expression was induced by heat shocking 2-d-old females at 38°C for 1 h to generate mutant clones and at 32.5°C for 30 min to generate Flip-out clones. Ectopic expression of *Hairless* (Johannes and Preiss, 2002) was performed by heat shocking (6 h before dissecting) 3–5-d-old females at 36.5°C for 1 h.

Follicle staining

Immunofluorescent staining of follicles was performed as described previously (Grammont and Irvine, 2001) using goat anti–β-galactosidase (1:1,000; Biogenesis), rabbit anti-Myc (1:100; Santa Cruz Biotechnology, Inc.), mouse anti-GFP (1:500; Sigma-Aldrich), rabbit anti-Zipper (1:1,000; Jordan and Karess, 1997), mouse anti-Eya (1:500; Developmental Studies Hybridoma Bank [DSHB]), mouse anti–α-tubulin (1:1,000; clone DM1A; Sigma-Aldrich), rat anti-ECad (1:200; DSHB), mouse anti-Armadillo (1:50; DSHB), and rat anti-NCad (1:20; DSHB) with the following modification: ovaries from females were dissected directly into fixative 5–7 d after Flipase induction (36 h for *sqh* mutant clones).

Description of the markers used

Follicles were staged according to King (1970) and Spradling (1993). MA33 is expressed only in the StCs from stage 9 onwards (Gonzalez-Reyes and St Johnston, 1998; Grammont and Irvine, 2002; Xi et al., 2003; Silver et al., 2005). *Dpp-lacZ* is also specifically expressed in the StCs at stage 9, as it turns on in some centripetal cells only at stage 10B (Dobens et al., 2000; Xi et al., 2003). Eya expression is specific at stage 9 to border and StC fates (Bai and Montell, 2002). In WT stage 9 follicles, the expression of these markers occurs progressively from the anterior part of the follicle and progresses posteriorly row by row as a wave. Accordingly, a gradient of expression for all of these markers is detected in the anterior part of a stage 9 follicle, with the strongest expression in the already flattened StCs, a weaker expression in the flattening StCs, and the weakest expression in cells that are about to undergo flattening. Because Eya is expressed in both border and StCs at stage 9, any conclusions drawn from an Eya staining were always confirmed with MA33, *dpp-lacZ*, or *Dad-lacZ* to avoid ambiguity concerning the fate of the cells. *Dad* was used as an StC fate marker because its expression pattern is similar to that of *dpp-lacZ* during stage 9. Surface areas of StCs were determined with LSM510 Meta software (Carl Zeiss MicroImaging, Inc.). Follicles were flattened under a coverslip such that the StCs in immediate contact with either the coverslip or the slide (i.e., those on the top or bottom of the follicle) could be viewed within a single focal plane. Only these StCs were used for surface area calculations to avoid inaccuracies caused by the natural curvature of the follicle, which was not taken into account.

Imaging

Confocal images were obtained using a microscope (LSM510 Meta; Carl Zeiss MicroImaging, Inc.) with 40× NA 1.3 plan-Neofluar and 63× NA 1.4 plan-Apochromat objectives. All imaging was performed at RT. Figures were processed using the LSM510 Meta software, Photoshop 7 (Adobe), and Freehand 10 (Macromedia). In all panels, unless otherwise stated, the focus is on the top plane, and a projection (z stack) of all of the z sections in which the StCs are visible is presented.

Online supplemental material

Fig. S1 shows that the Armadillo expression pattern mirrors AJ remodeling and shows the expression of Armadillo in WT follicles and in *Dl Ser* mutant follicles. Fig. S2 shows that AJ remodeling in *fng* mutant follicles is delayed but not blocked and shows the expression of ECad in stage 10A *fng* mutant follicles. Fig. S3 shows that StC flattening and AJ remodeling required transcriptional activity of the Notch pathway and shows the expression of *Dl-lacZ*, *E(spl)mβ7-lacZ*, and *E(spl)mβ-CD2* reporters in stage 9 follicles as well as the delay in AJ remodeling observed in stage 9 follicles overexpressing *Hairless* and in stage 9 follicles overexpressing Nact. Fig. S4 shows that *shg* controls the down-regulation of NCad and shows the expression of NCad in *shg* mutant clones at stages 7 and 8. Online supplemental material is available at http://www.jcb.org/cgi/content/full/jcb.200609079/DC1.

I thank R. Karess, L. Dobens, D. Godt, A. Preiss, F. Schweisguth, K. Irvine, the DSHB, and the Bloomington Stock Center for antibodies and *Drosophila* stocks and R. Karess, D. Godt, K. Irvine, F. Schweisguth, C. Vachias, O. Bardot, J.L. Couderc, and P. Das for helpful remarks and comments on the manuscript.

This research was supported by the Institut National de la Santé et de la Recherche Médicale.

Submitted: 13 September 2006
Accepted: 9 March 2007

References

Bai, J., and D. Montell. 2002. Eyes absent, a key repressor of polar cell fate during *Drosophila* oogenesis. *Development*. 129:5377–5388.

Beccari, S., L. Teixeira, and P. Rorth. 2002. The JAK/STAT pathway is required for border cell migration during *Drosophila* oogenesis. *Mech. Dev.* 111:115–123.

Bertet, C., L. Sulak, and T. Lecuit. 2004. Myosin-dependent junction remodelling controls planar cell intercalation and axis elongation. *Nature*. 429:667–671.

Cooper, M.T., and S.J. Bray. 1999. Frizzled regulation of Notch signalling polarizes cell fate in the *Drosophila* eye. *Nature*. 397:526–530.

de Celis, J.F., R. Barrio, A. del Arco, and A. Garcia-Bellido. 1993. Genetic and molecular characterization of a Notch mutation in its Delta- and Serrate-binding domain in *Drosophila*. *Proc. Natl. Acad. Sci. USA*. 90:4037–4041.

Deng, W.M., C. Althauser, and H. Ruohola-Baker. 2001. Notch-Delta signaling induces a transition from mitotic cell cycle to endocycle in *Drosophila* follicle cells. *Development*. 128:4737–4746.

Dobens, L.L., and L.A. Raftery. 2000. Integration of epithelial patterning and morphogenesis in *Drosophila* ovarian follicle cells. *Dev. Dyn.* 218:80–93.

Dobens, L.L., J.S. Peterson, J. Treisman, and L.A. Raftery. 2000. *Drosophila* bunched integrates opposing DPP and EGF signals to set the operculum boundary. *Development*. 127:745–754.

Dobens, L., A. Jaeger, J.S. Peterson, and L.A. Raftery. 2005. Bunched sets a boundary for Notch signaling to pattern anterior eggshell structures during *Drosophila* oogenesis. *Dev. Biol.* 287:425–437.

Doherty, D., G. Feger, S. Younger-Shepherd, L.Y. Jan, and Y.N. Jan. 1996. Delta is a ventral to dorsal signal complementary to Serrate, another Notch ligand, in *Drosophila* wing formation. *Genes Dev.* 10:421–434.

Godt, D., and U. Tepass. 1998. *Drosophila* oocyte localization is mediated by differential cadherin- based adhesion. *Nature*. 395:387–391.

Gonzalez-Reyes, A., and D. St Johnston. 1998. Patterning of the follicle cell epithelium along the anterior-posterior axis during *Drosophila* oogenesis. *Development*. 125:2837–2846.

Gonzalez-Reyes, A., H. Elliott, and R.D. St Johnston. 1995. Polarization of both major body axes in *Drosophila* by gurken-torpedo signalling. *Nature*. 375:654–658.

Gonzalez-Reyes, A., H. Elliott, and D. St Johnston. 1997. Oocyte determination and the origin of polarity in *Drosophila*: the role of the spindle genes. *Development*. 124:4927–4937.

Grammont, M., and K.D. Irvine. 2001. fringe and Notch specify polar cell fate during *Drosophila* oogenesis. *Development*. 128:2243–2253.

Grammont, M., and K.D. Irvine. 2002. Organizer activity of the polar cells during *Drosophila* oogenesis. *Development*. 129:5131–5140.

Grossniklaus, U., H.J. Bellen, C. Wilson, and W.J. Gehring. 1989. P-element-mediated enhancer detection applied to the study of oogenesis in *Drosophila*. *Development*. 107:189–200.

Heitzler, P., and P. Simpson. 1991. The choice of cell fate in the epidermis of *Drosophila*. *Cell*. 64:1083–1092.

Horne-Badovinac, S., and D. Bilder. 2005. Mass transit: epithelial morphogenesis in the *Drosophila* egg chamber. *Dev. Dyn.* 232:559–574.

Irvine, K.D., and E. Wieschaus. 1994. fringe, a boundary-specific signaling molecule, mediates interactions between dorsal and ventral cells during *Drosophila* wing development. *Cell*. 79:595–606.

Ito, K., H. Sass, J. Urban, A. Hofbauer, and S. Schneuwly. 1997. GAL4-responsive UAS-tau as a tool for studying the anatomy and development of the *Drosophila* central nervous system. *Cell Tissue Res.* 290:1–10.

Jiang, J., and G. Struhl. 1995. Protein kinase A and hedgehog signaling in *Drosophila* limb development. *Cell*. 80:563–572.

Johannes, B., and A. Preiss. 2002. Wing vein formation in *Drosophila melanogaster*: hairless is involved in the cross-talk between Notch and EGF signaling pathways. *Mech. Dev.* 115:3–14.

Jordan, P., and R. Karess. 1997. Myosin light chain-activating phosphorylation sites are required for oogenesis in *Drosophila*. *J. Cell Biol.* 139:1805–1819.

Kai, T., and A. Spradling. 2003. An empty *Drosophila* stem cell niche reactivates the proliferation of ectopic cells. *Proc. Natl. Acad. Sci. USA*. 100:4633–4638.

Karess, R.E., X.J. Chang, K.A. Edwards, S. Kulkarni, I. Aguilera, and D.P. Kiehart. 1991. The regulatory light chain of nonmuscle myosin is encoded by spaghetti-squash, a gene required for cytokinesis in *Drosophila*. *Cell*. 65:1177–1189.

Keller Larkin, M., W.M. Deng, K. Holder, M. Tworoger, N.J. Clegg, and H. Ruohola-Baker. 1999. Role of Notch pathway in terminal follicle cell differentiation during *Drosophila* oogenesis. *Dev. Genes Evol.* 209:301–311.

King, R.C. 1970. Ovarian Development in *Drosophila melanogaster*. Academic Press, New York. 227 pp.

Lohs-Schardin, M. 1982. Dicephalic—a *Drosophila* mutant affecting polarity in follicle organization and embryonic patterning. *Roux Arch. dev. Biol.* 191:28–36.

Lopez-Schier, H., and D. St Johnston. 2001. Delta signaling from the germ line controls the proliferation and differentiation of the somatic follicle cells during *Drosophila* oogenesis. *Genes Dev.* 15:1393–1405.

Niewiadomska, P., D. Godt, and U. Tepass. 1999. DE-Cadherin is required for intercellular motility during *Drosophila* oogenesis. *J. Cell Biol.* 144:533–547.

Roth, S., F.S. Neuman-Silberberg, G. Barcelo, and T. Schupbach. 1995. cornichon and the EGF receptor signaling process are necessary for both anterior-posterior and dorsal-ventral pattern formation in *Drosophila*. *Cell*. 81:967–978.

Royou, A., W. Sullivan, and R. Karess. 2002. Cortical recruitment of nonmuscle myosin II in early syncytial *Drosophila* embryos: its role in nuclear axial expansion and its regulation by Cdc2 activity. *J. Cell Biol.* 158:127–137.

Silver, D.L., and D.J. Montell. 2001. Paracrine signaling through the JAK/STAT pathway activates invasive behavior of ovarian epithelial cells in *Drosophila*. *Cell*. 107:831–841.

Silver, D.L., E.R. Geisbrecht, and D.J. Montell. 2005. Requirement for JAK/STAT signaling throughout border cell migration in *Drosophila*. *Development*. 132:3483–3492.

Spradling, A.C. 1993. Development genetics of oogenesis. *In* The Development of *Drosophila melanogaster*. M. Bate and A. Martinez-Arias, editors. Cold Spring Harbor Laboratory Press, Cold Spring Harbor, NY. 1–70.

Sun, X., and S. Artavanis-Tsakonas. 1996. The intracellular deletions of Delta and Serrate define dominant negative forms of the *Drosophila* Notch ligands. *Development*. 122:2465–2474.

Torres, I.L., H. Lopez-Schier, and D. St Johnston. 2003. A Notch/Delta-dependent relay mechanism establishes anterior-posterior polarity in *Drosophila*. *Dev. Cell*. 5:547–558.

Xi, R., J.R. McGregor, and D.A. Harrison. 2003. A gradient of JAK pathway activity patterns the anterior-posterior axis of the follicular epithelium. *Dev. Cell*. 4:167–177.

Xu, T., and G.M. Rubin. 1993. Analysis of genetic mosaics in developing and adult *Drosophila* tissues. *Development*. 117:1223–1237.

Zarnescu, D.C., and G.H. Thomas. 1999. Apical spectrin is essential for epithelial morphogenesis but not apicobasal polarity in *Drosophila*. *J. Cell Biol.* 146:1075–1086.

Zhao, D., D. Clyde, and M. Bownes. 2000. Expression of fringe is down regulated by Gurken/Epidermal Growth Factor Receptor signalling and is required for the morphogenesis of ovarian follicle cells. *J. Cell Sci.* 113:3781–3794.